Title

Noninvasive monitoring of hemodynamic stress using quantitative near-infrared frequency-domain photon migration spectroscopy

Journal

Journal of Biomedical Optics, 7(1)

ISSN

1083-3668

Authors

Pham, Tuan H

Hornung, Rene

Ha, Hongphuc P

et al.

Publication Date

2002

DOI

10.1117/1.1427046

Journal of Biomedical Optics 7(1), 34–44 (January 2002)

Noninvasive monitoring of hemodynamic stress using quantitative near-infrared frequency-domain photon migration spectroscopy

Tuan H. Pham
University of California
Beckman Laser Institute and Medical Clinic
Irvine, California

René Hornung
University of California
Beckman Laser Institute and Medical Clinic
Irvine, California
and
University Hospital Zurich
Department of Obstetrics and Gynecology
Zurich, Switzerland

Hongphuc P. Ha
Tanya Burney
University of California
Beckman Laser Institute and Medical Clinic
Irvine, California

Dan Serna
Ledford Powell
University of California College of Medicine
Department of Pulmonary Medicine and Cardiothoracic Surgery
Irvine, California

Matthew Brenner
University of California
Beckman Laser Institute and Medical Clinic
Irvine, California
and
University of California College of Medicine
Department of Pulmonary Medicine and Cardiothoracic Surgery
Irvine, California

Bruce J. Tromberg
University of California
Beckman Laser Institute and Medical Clinic
Irvine, California

Abstract. Hemorrhagic hypovolemia and inotropic agent administration were used to manipulate cardiac output (CO) and oxygen delivery in rabbits to investigate the correlation between noninvasive frequency domain photon migration (FDPM) spectroscopy and invasive hemodynamic monitoring parameters. Frequency-domain photon migration provides quantitative measurements of light absorption and reduced scattering (μ_a and μ_s', respectively) in tissue. Wavelength dependent μ_a values were used to calculate *in vivo* tissue concentration of deoxyhemoglobin [Hb], oxyhemoglobin [HbO_2], total hemoglobin [TotHb], and water [H_2O] as well as mixed arterial-venous oxygen saturation (S_tO_2) in tissue. FDPM-derived physiologic properties were correlated with invasive measurements of CO and mean pulmonary artery pressure (mPAP), FDPM-derived [TotHb] and S_tO_2 correlated significantly with hemorrhaged volume (HV), mPAP, and CO. Correlation coefficients for [TotHb] vs HV, mPAP, and CO were −0.77, 0.86, and 0.70, respectively. Correlation coefficients of S_tO_2 vs HV, mPAP, and CO were −0.71, 0.55, and 0.61, respectively. Dobutamine induced changes resulted in correlation coefficients between FDPM-derived and invasively measured physiologic parameters that are comparable to those induced by hypovolemia. FDPM spectroscopy is sensitive to changes in mPAP and CO of as little as 15%. These results suggest that FDPM spectroscopy may be used in clinical settings to noninvasively monitor central hemodynamic parameters and to directly assess oxygenation of tissues. [DOI: 10.1117/1.1427046]

Keywords: hemoglobin; hypovolemia; tissue optical properties; shock; tissue oxygenation.

Paper JBO-102104 received Apr. 6, 2001; revised manuscript received Aug. 7, 2001; accepted for publication Aug. 20, 2001.

1 Introduction

Adequate perfusion and oxygenation are critical for tissue viability. Insufficient tissue oxygenation is the underlying cause of tissue damage for an extensive range of medical emergencies, e.g., hypovolemic shock, peripheral vascular disease, and stroke. Tissue oxygenation depends on oxygen delivery (DO_2) as well as oxygen consumption (VO_2). DO_2 is a product of cardiac output (CO) and arterial oxygen content and is an accurate indicator of the overall oxygenation status of the body.[1,2] Regional oxygen delivery depends on DO_2 and the local vascular resistance, while VO_2 is the difference between arterial delivery and venous return of oxygen {i.e., $VO_2 = CO x([aO_2]-[vO_2])$}. Since arterial $[aO_2]$ and venous $[vO_2]$ oxygen contents are generally proportional to hemoglobin oxygen saturation, DO_2 and VO_2 usually correlate to arterial (S_aO_2) and venous (S_vO_2) oxygen saturation and cardiac output. Hemodynamic monitoring of DO_2 and VO_2 is a widely accepted principle for managing various medical emergencies, particularly circulatory dysfunction and shock.[1,3–5] Noninvasive arterial blood pressure and heart rate are considered to be poor indicators of early shock.[4,6]

Pulmonary artery thermodilution and Swan–Ganz catheterization to determine CO and pulmonary artery wedge pressure (PWP) are common invasive clinical procedures to measure DO_2 and VO_2 that may cause serious complications. While DO_2 and VO_2 are accurate indicators of the overall oxygenation status of the body, they are not necessarily representative of regional tissue oxygenation. The fractional distribution of CO to various organs is cumbersome if not im-

Address all correspondence to Bruce J. Tromberg, PhD. Tel: 949-824-6996; Fax: 949-824-2726; E-mail: tromberg@bli.uci.edu

1083-3668/2002/$15.00 © 2002 SPIE

possible to determine, especially in vasculature with multiple arterial supplies and instances of regional heterogeneity. A noninvasive modality capable of quantifying local tissue oxygenation that is also sensitive to factors contributing to DO_2 and VO_2 is of clinical importance for monitoring tissue hypoxia secondary only to shock.

Several noninvasive optical techniques are currently under investigation, including laser Doppler imaging[7] and near-infrared (NIR) reflectance.[8–11] The methodology and merits of NIR spectroscopy have been intensely examined by numerous researchers.[12–16] Substantial progress has been made during the past decade in our ability to quantify tissue optical and physiologic properties, largely due to the emergence of time and frequency-domain photon migration techniques.[11,17] Frequency-domain photon migration (FDPM) uses high frequency (MHz–GHz) intensity modulated near-infrared light to noninvasively quantify light absorption (μ_a) and reduced scattering (μ_s') parameters in tissue. μ_a and μ_s' are sensitive to biologically important light-absorbing and -scattering molecules and structures. Intrinsic NIR absorbers in tissue are generally assumed to be hemoglobin [deoxy-(Hb) and oxy-(HbO_2)], water (H_2O), fat, cytochromes, and melanin.[18,19] Quantitative measurements of wavelength-dependent light absorption can be used to determine the *in vivo* concentrations of these species. Additional parameters such as tissue blood volume fraction, hemoglobin oxygen saturation (S_tO_2), and oxygen utilization can be deduced. Note that, in this article, the term tissue oxygenation (S_tO_2) refers to the oxygenation of arteriovenous hemoglobin found within vessels that have diameters ranging from capillaries to medium-size veins/arteries. Although S_tO_2 and oxygen partial pressure (tension) are proportional, they are distinct quantities. Light scatterers are cellular (e.g., organelles, proteins) and extracellular (e.g., collagen, elastin) tissue components.[20,21] Measurements of wavelength-dependent scattering properties offer insight into the composition, density, and organization of tissue structures. Consequently, changes in wavelength-dependent scattering properties may accompany processes such as ischemia, necrosis, wound healing, and malignancy.

The sensitivity of optical properties to the tissue's functional and structural components may provide a means for noninvasive assessment of pathophysiologic processes, such as ischemia and hypoxia. Indeed, previous studies have shown significant changes in the tissue's optical and physiologic properties in response to local ischemia.[17,22,23] In this pilot study, substantial hemodynamic changes were induced in a rabbit model to investigate how changes in DO_2 affect tissue oxygenation of the limb. The aim of this study was to assess (1) the feasibility of using FDPM spectroscopy to quantify local tissue oxygenation and (2) the sensitivity of FDPM-derived parameters to changes in tissue oxygenation due to perturbation in DO_2.

2 Materials and Methods

Experimental setups based on hypovolemia and dobutamine treatment were selected on the basis of clinical relevance. Hypovolemia was induced in the rabbit in order to decrease CO, and thereby decrease DO_2. Dobutamine was administered to increase CO and DO_2. FDPM data were collected concurrently with systemic hemodynamic parameters, specifically, CO, mean pulmonary artery pressure (mPAP), arterial saturation (S_aO_2), and mean systemic arterial pressure (mSAP). FDPM-derived physiologic properties were correlated to hemodynamic parameters.

2.1 Animal

Pathogen-free white New Zealand male rabbits (Myrtle Rabbitry Inc., Thompson Station, TN), weighing 4.0 [$\pm$0.4 standard deviation (SD)] kg, were used. Animals were housed in a pathogen-free animal facility and were given a commercial basal diet and water *ad libitum*. The study was approved by the Institutional Laboratory Animal Care and Use Committee, University of California, Irvine (ARC protocol No. 97-1556).

2.2 Procedures

Hypovolemic hemorrhagic shock was induced in six animals (the hypovolemic group). Dobutamine was administered to another six animals (the dobutamine group). The animals were anesthetized by an intramuscular injection of a ketamine–xylazine mixture at an induction dose of 50 mg/kg ketamine (Ketaject, Phoenix Pharmaceutical Inc., St. Joseph, MI) and 5 mg/kg xylazine (Anased, Lloyd Laboratories, Shenandoah, IA). Anesthesia was maintained as needed by intravenous administration of the ketamine–xylazine mixture at doses of 2.5–5.0 mg/kg ketamine and 0.5–1.0 mg/kg xylazine. Immediately following anesthesia induction, animals were intubated using a size 3.0 endotracheal tube and mechanically ventilated (dual phase control respirator, model 32A4BEPM-5R, Harvard Apparatus, Chicago, IL) at a respiration rate of 32/min and a tidal volume of 50 cc at 100% inspiratory oxygen. The animals were shaved at the thorax and thighs. The chest wall was opened to expose the thoracic cavity, allowing direct access to the heart and aorta. The animals were euthanized by exsanguination immediately after the study in accordance with federal guidelines.

2.3 Physiology Measurements

A calibrated flow transducer (T106 small animal flow meter, Transonic System, Inc., Ithaca, NY) was placed around the ascending aorta to measure CO. A time trace of the cardiac flow was recorded for ~10 s, and an average of the time of the flow profile was calculated to yield the mean amount of CO. The heart rate (HR) was also determined from the time profile of cardiac flow. To measure the pulmonary arterial pressure, a calibrated pressure transducer (TSD104A transducer and MP100 WSW System, Biopac Systems, Inc., Santa Barbara, CA) was connected to a fluid-filled line terminated by an 18 gauge catheter. The catheter was inserted directly into the right ventricular chamber and advanced into the pulmonary artery under continuous monitoring for the duration of the measurement. A time trace of the pulmonary arterial pressure was recorded for 10 s. The systolic and diastolic pressures corresponded to the peak and trough of the pressure profile; the mPAP was calculated digitally. Systemic arterial pressures were similarly measured, with the transducer-connected catheter inserted into the ear artery. The mSAP was recorded.

Blood was drawn from the artery of the ear for arterial blood gas chemistry. All fluid-filled lines connected to the transducers were intermittently flushed with small volumes

(<1/2 cc) of heparin to prevent blood clots. A pulse oximeter probe (Biox 3700 pulse oximeter, Ohmeda, Hurst, TX) was placed on the forelimb to measure the S_aO_2 and HR. Baseline values for all hemodynamic and noninvasive measurements were determined prior to induction of hypovolemia or administration of dobutamine.

2.4 Hypovolemia

An 18-gauge needle was inserted into the right atrium and 5 cc of hemorrhaged volume (HV) was slowly removed. Three minutes later, hemodynamic parameters were measured again in conjunction with FDPM spectroscopy. The procedure was repeated until a total HV of 60 cc (corresponding to an average of 42% of the total blood volume) was removed, except for in one rabbit where a total volume of 120 cc was removed.

2.5 Dobutamine Administration

Dobutamine doses of 30, 40, and 50 μg/kg were sequentially administered into the ear vein at a average rates of 40, 53, and 67 μg/min, respectively. One minute after each dose, the hemodynamic parameters were measured simultaneously with the FDPM measurements. Two trials of administration of dobutamine were carried out on each rabbit. The values obtained from the two trials were averaged.

2.6 FDPM

Theory and instrumentation of the FDPM approach to quantify tissue optical properties are described in detail elsewhere.[24,25] Briefly, FDPM launches sinusoidally intensity modulated NIR light into highly scattering tissues. Light that is sinusoidally intensity modulated at angular frequency ω propagates in tissues as highly damped diffuse photon-density waves (PDWs) with well-defined wave characteristics, specifically, the phase velocity and decay rate.[26] PDW propagation depends on the bulk tissue optical properties and can be described by a diffusion approximation for light transport in turbid media, e.g., tissues.

Analytically derived solutions to the diffusion equation for the semi-infinite boundary condition yield nonlinear PDW model functions. The model functions are fit to measurements of the frequency-dependent phase shift and amplitude attenuation of diffusely reflected PDWs in order to explicitly calculate tissue μ_a and μ_s'. Wavelength-dependent absorption is used to determine the tissue concentration of deoxyhemoglobin [Hb], oxyhemoglobin [HbO_2], [TotHb] (=[Hb] +[HbO_2]), S_tO_2=([HbO_2]/[TotHb]x100%), and water [H_2O]; throughout this article, these abbreviations refer to values derived from FDPM measurements. The tissue concentrations and absorption values are related through molar extinction coefficients, ε, by the

$$\begin{bmatrix} \mu_{674} \\ \mu_{798} \\ \mu_{811} \\ \mu_{849} \\ \mu_{956} \end{bmatrix} = \begin{bmatrix} \varepsilon_{Hb}^{674} & \varepsilon_{HbO_2}^{674} & \varepsilon_{H_2O}^{674} \\ \varepsilon_{Hb}^{798} & \varepsilon_{HbO_2}^{798} & \varepsilon_{H_2O}^{798} \\ \varepsilon_{Hb}^{811} & \varepsilon_{HbO_2}^{811} & \varepsilon_{H_2O}^{811} \\ \varepsilon_{Hb}^{849} & \varepsilon_{HbO_2}^{849} & \varepsilon_{H_2O}^{849} \\ \varepsilon_{Hb}^{956} & \varepsilon_{HbO_2}^{956} & \varepsilon_{H_2O}^{956} \end{bmatrix} \begin{bmatrix} [Hb] \\ [HbO_2] \\ [H_2O] \end{bmatrix}. \quad (1)$$

Extinction coefficients for Hb, HbO_2, and H_2O were obtained from published values.[18] Least-squares fits were used to solve Eq. (1), with the constraint that the concentration values must be greater than zero.[27]

For this study, a portable broad-bandwidth FDPM instrument was used to quantify tissue optical properties at multiple NIR wavelengths. FDPM measurements were performed using a probe with a source–detector separation of 9.45 mm. Both the source and detecting fibers were gently placed on the quadricep muscles to collect the FDPM data set, which consists of phase and amplitude data for the wavelengths at 674, 798, 811, 849, and 956 nm. The quadricep muscles were chosen because of their large tissue mass and thus best fulfill the semi-infinite boundary condition. Each data set consists of three to four repetitive measurements. Figure 1 is a schematic of the setup used to perform FDPM and hemodynamic measurements.

2.7 Data Analysis

Baseline data from the hypovolemic (six rabbits) and dobutamine (six rabbits) group were combined, i.e., hemodynamic- and FDPM-derived data on the 12 rabbits were pooled. Mean and standard deviation (±SD) were calculated from the pooled baseline values for CO, mPAP, mSAP, and FDPM-derived optical and physiologic parameters.

In order to compare data obtained from different animals, the percentages of change from baseline values were computed for CO, mPAP, mSAP, and FDPM-derived physiologic concentrations. The percentages of change for CO, mPAP, mSAP, [Hb], [HbO_2], [TotHb], [S_tO_2], and [H_2O] from the hypovolemic group were combined. The percentages of change in the FDPM-derived physiologic parameters were correlated to HV, ΔCO, and ΔmPAP. To quantify the extent of association between these variables, the correlation coefficient and the 95% confidence interval were computed. Data from the dobutamine-treated group were analyzed in the same manner.

3 Results

3.1 Hemodynamic Measurements

Values of CO, mPAP, and mSAP were measured for each incremental HV or dobutamine dose. Figures 2(a) and 2(b) show typical time traces of the cardiac flow and pulmonary arterial pressure, respectively. HR and CO were determined from the time trace of the cardiac flow, and mPAP was determined from time trace of pulmonary arterial pressure. The mean systemic arterial pressure was recorded. Baseline values for CO, mPAP, and mSAP from the hypovolemic- and dobutamine-treated groups were combined and are summarized in Table 1.

3.2 FDPM

An example of the FDPM phase and amplitude data is shown Figure 3(a) for 798 nm. Model functions were fit to the phase (□, left y axis) and amplitude (♦, right y axis) of the PDW to determine the tissues' optical properties. Model functions (lines) fit the phase and amplitude data well and yielded μ_a and μ_s' values. Representative μ_a (□, left y axis) and μ_s' (♦, right y axis) of the five wavelengths are shown in Figure 3(b).

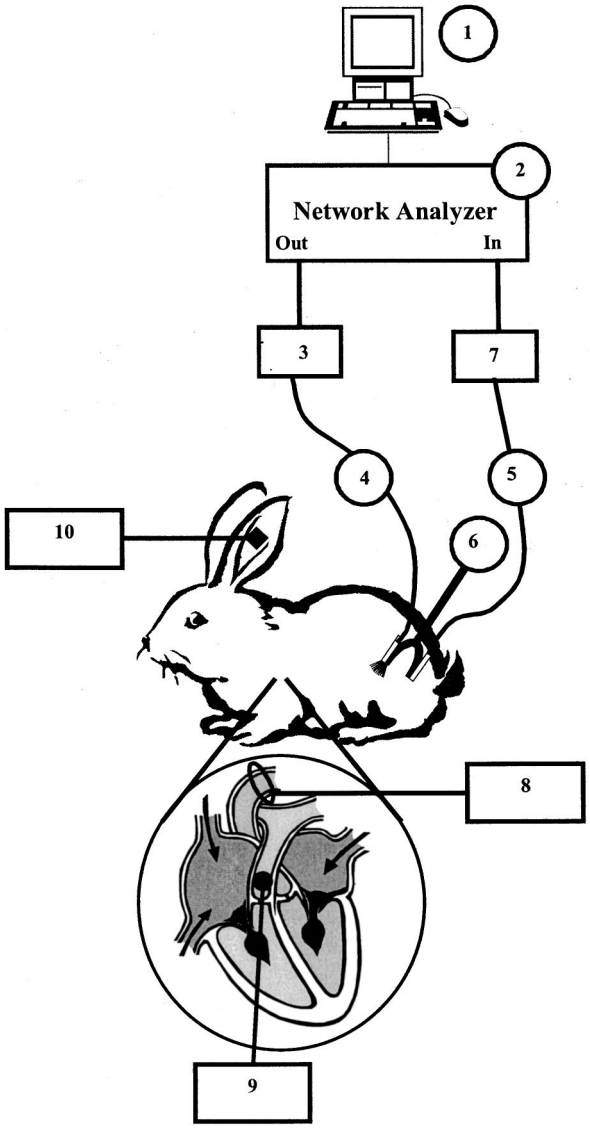

Fig. 1 Schematic showing FDPM spectroscopy in conjunction with measurements of hemodynamic parameters. The FDPM instrument consists of the following principal components: computer (1), network analyzer (2), five NIR diode lasers (3) at 674, 798, 811, 849, and 956 nm, optical fiber for the light source (4) and signal detection (5) mounted 9.45 mm apart on a probe (6), and an avalanche photodiode (7). The probe was placed gently on the shaved area of the hind limb. CO was measured using a calibrated flow transducer (8) placed around the aorta. PAP and SAP were measured with pressure transducers placed, respectively, in the right ventricle and advanced into the pulmonary artery (9) and in the artery of the ears (10). S_aO_2 was initially determined from and arterial blood gas analysis and subsequently monitored with a pulse oximeter placed on the forelimb.

Also shown is a line that represents a least-squares fit to the wavelength-dependent μ_a values, resulting in $[Hb] = 25.8\,\mu M$, $[HbO_2] = 49.6\,\mu M$, $[TotHb] = 75.4\,\mu M$, $S_tO_2 = 65.8\%$, and $[H_2O] = 31.6\,M$ for the specific data set shown in Figure 3. Table 2 summarizes the baseline optical properties of the five wavelengths used, and Table 3 summarizes the baseline FDPM-derived physiologic properties.

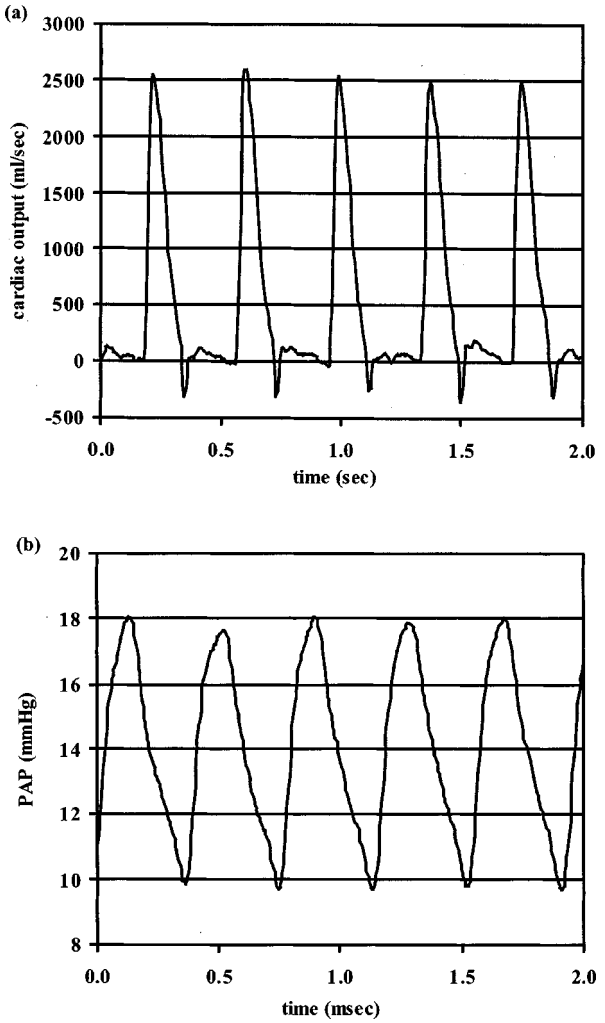

Fig. 2 (a) Example showing the time trace of the cardiac flow, collected with a calibrated flow transducer placed around the aorta. The time average of the cardiac flow is the mean cardiac output. The heart rate is also determined from the cardiac flow time profile. (b) Time trace of the pulmonary artery pressure. A needle, which was connected to the transducer, was inserted into the right atrium in order to measure PAP. Systolic and diastolic PAP correspond to the peak and trough, respectively. An average of the systolic and diastolic PAP gives the mean PAP.

3.3 Hypovolemia

Figure 4 shows a representative example of the progression of physiologic parameters as a function of the increasing severity

Table 1 Mean and standard deviation of CO, mPAP, and mSAP.

Physiologic parameters	Mean±SD[a]
CO	394±61 mL/min
mPAP	12±3 mm Hg
mSAP	80±13 mm Hg

[a] Calculated from baseline data in hypovolemic and dobutamine groups, $n = 12$.

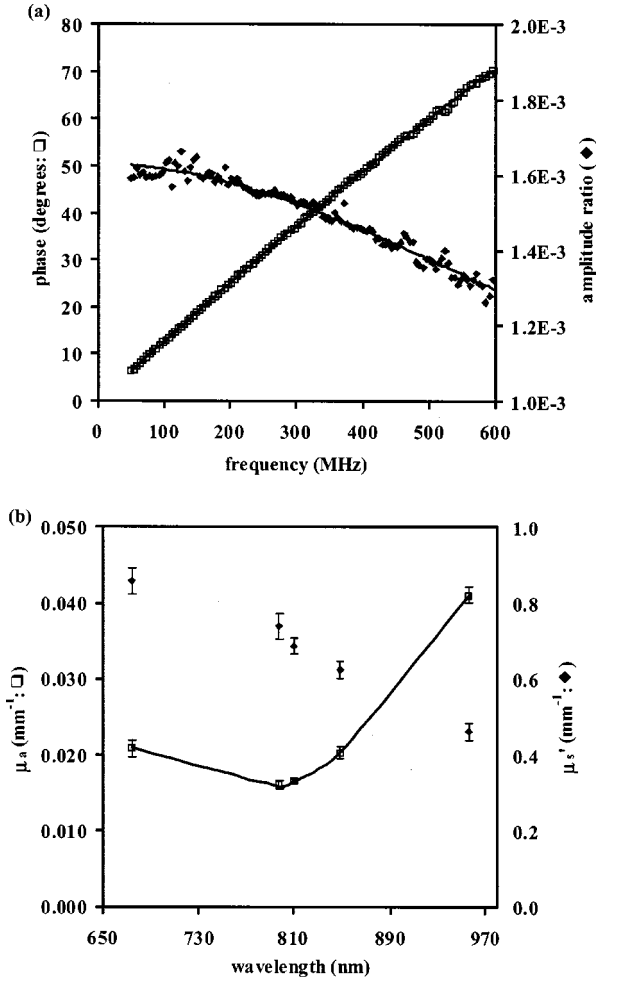

Fig. 3 (a) Example of FDPM phase (□, left *y* axis) and amplitude (◆, right *y* axis) data at 798 nm collected from the tissues of the rabbit's hind limb. Model functions are fit to FDPM phase and amplitude data to extract tissue μ_a and μ_s'. Lines represent results of fitting the model functions to the data. (b) Representative tissue μ_a (□, left *y* axis) and μ_s' (◆, right *y* axis) for the five wavelengths. The μ_a and μ_s' for each wavelength were extracted from the FDPM phase and amplitude at that wavelength. A constraint-imposed least-squares solution to Eq. (1) is obtained for the wavelength-dependent μ_a data in order to calculate [Hb], [HbO_2], and [H_2O]. The solid line through the μ_a data represents the least-squares fits.

of hypovolemia. In Figure 4(a), CO (◆, left *y* axis) and mPAP (□, right *y* axis) started to decrease when as little as 10 mL (~7% total blood volume) of blood was removed, while mSAP (■, right *y* axis) remained relatively constant until the HV reached ~30 mL (~21% of the total blood volume). Figure 4(b) is a plot of FDPM-derived concentrations for Hb (□, left *y* axis), HbO_2 (■, left *y* axis), and H_2O (◆, right *y* axis) versus HV. Figure 4(c) is a plot of TotHb (□, left *y* axis) and mixed S_tO_2 saturation (◆, right *y* axis) versus HV. As was observed with CO and mPAP values, [HbO_2], [TotHb], and S_tO_2 significantly decrease when as little as 10–15 mL of blood is removed. Interestingly, [Hb] and [H_2O] remained relatively constant even when the hemorrhage volume reached 60 mL (~42% of the total blood volume).

For each animal in the hypovolemic group, we calculated the percentages of change from the baseline values for the

Table 2 Mean and standard deviation of FDPM-measured tissue optical properties.

Wavelength (nm)	μ_a mean±SD[a] (mm^{-1})	μ_s' mean±SD[a] (mm^{-1})
674	0.0194±0.0012	1.00±0.12
798	0.0148±0.0009	0.86±0.09
811	0.0146±0.0011	0.77±0.05
849	0.0186±0.0011	0.71±0.06
956	0.0383±0.0012	0.57±0.07

[a] Calculated from baseline data pooled from hypovolemic and dobutamine-treated groups, $n=158$.

hemodynamic- and FDPM-derived physiologic parameters in response to blood loss. The percentage of change data on all animals in the hypovolemic group were combined. To ascertain that acute hemorrhaging decreased mPAP and CO, we determined the correlation coefficients for ΔmPAP vs HV and ΔCO vs HV. Correlation coefficients of −0.76 and −0.82 were obtained for ΔmPAP vs HV and for ΔCO vs HV, respectively. The mean PAP and CO decreased by as much as 50% and 80%, respectively, in response to blood loss of 60 cc. Correlations between Δ[TotHb] vs HV, Δ[TotHb] vs ΔmPAP, and Δ[TotHb] vs ΔCO are shown for the hemorrhaged group in Figures 5(a)–5(c), respectively. Δ[TotHb] is seen to be correlated with HV, ΔmPAP, and ΔCO, resulting in correlation coefficients of −0.77, 0.68, and 0.70, respectively. Furthermore, the [TotHb] measured decreased approximately 10% in response to 60 mL of blood loss, while mPAP decreased 50%, and CO decreased 80%.

Figures 6(a)–6(c) illustrate the relationship of changes in tissue hemoglobin oxygen saturation (ΔS_tO_2) and HV, ΔmPAP, and ΔCO, respectively. As shown Figure 6, ΔS_tO_2 varies with each, resulting in correlation coefficients of −0.71, 0.55, and 0.61, respectively. As indicated by the smaller magnitude of the correlation coefficients, the association among HV, ΔmPAP, and ΔCO vs ΔS_tO_2 is less dramatic than these parameters versus [TotHb]. Table 4 summarizes the

Table 3 Mean and standard deviation of FDPM-derived physiologic properties.

FDPM-derived physiologic properties	Mean±SD[a]
[Hb]	24.3±1.6 μM
[HbO_2]	44.9±4.4 μM
[TotHb]	69.2±5.9 μM
S_tO_2	64.8%±5.3%
[H_2O]	30.2±2.2 M

[a] Calculated using baseline data pooled from both the hypovolemia and dobutamine-treated groups, $n=177$.

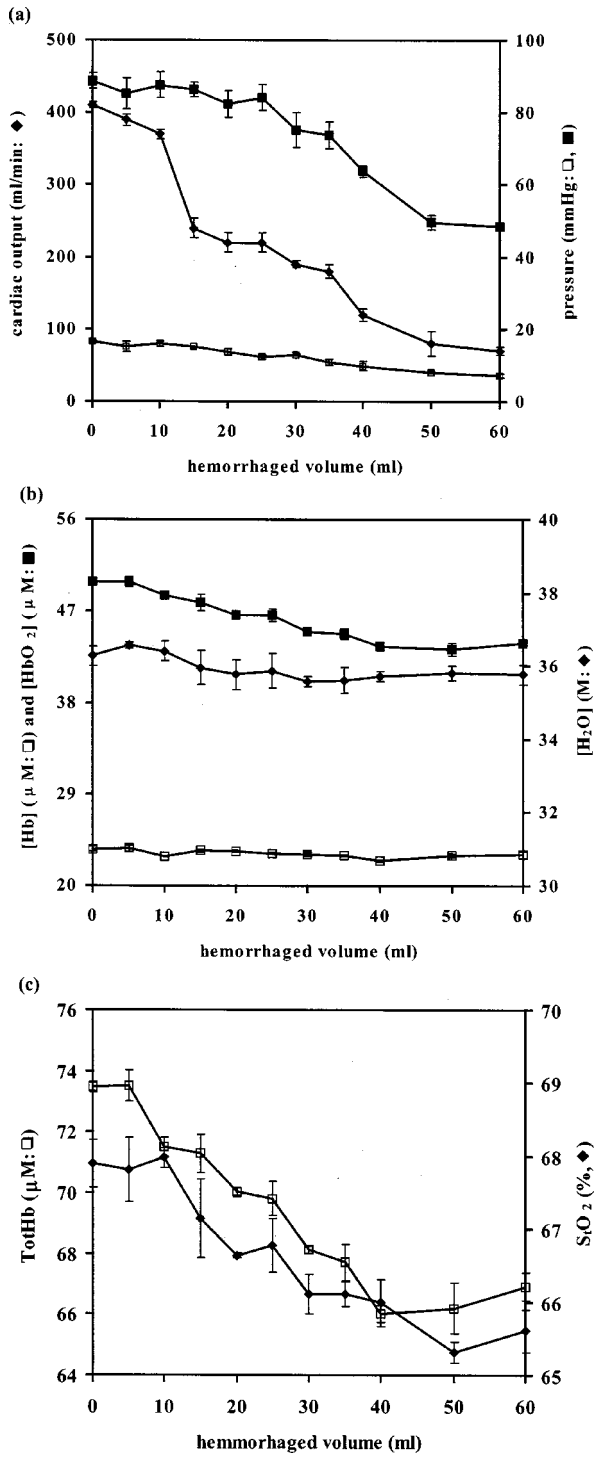

Fig. 4 Representative data for the dependence of physiologic as well as FDPM-derived parameters on the hemorrhaged volume. Data points represent mean values and error bars are standard deviations. (a) CO (◆, left *y* axis), mPAP (□, right *y* axis), and mSAP (■, right *y* axis) are plotted vs HV. CO and mPAP start to decrease when as little as 10 mL of blood is lost, while mSAP remains constant until the blood loss exceeds 30 mL. (b) FDPM-derived tissue concentrations vs HV: Hb (□, left *y* axis), HbO_2 (■, left *y* axis), and [H_2O] (◆, right *y* axis). [HbO_2] decreases with the hemorrhaged volume, while [Hb] and [H_2O] remain relatively constant. (c) [TotHb] (□, left *y* axis) and mixed S_tO_2 (◆, right *y* axis) plotted as a function of HV. [TotHb] and S_tO_2 decrease in response to blood loss of as little as 10 mL.

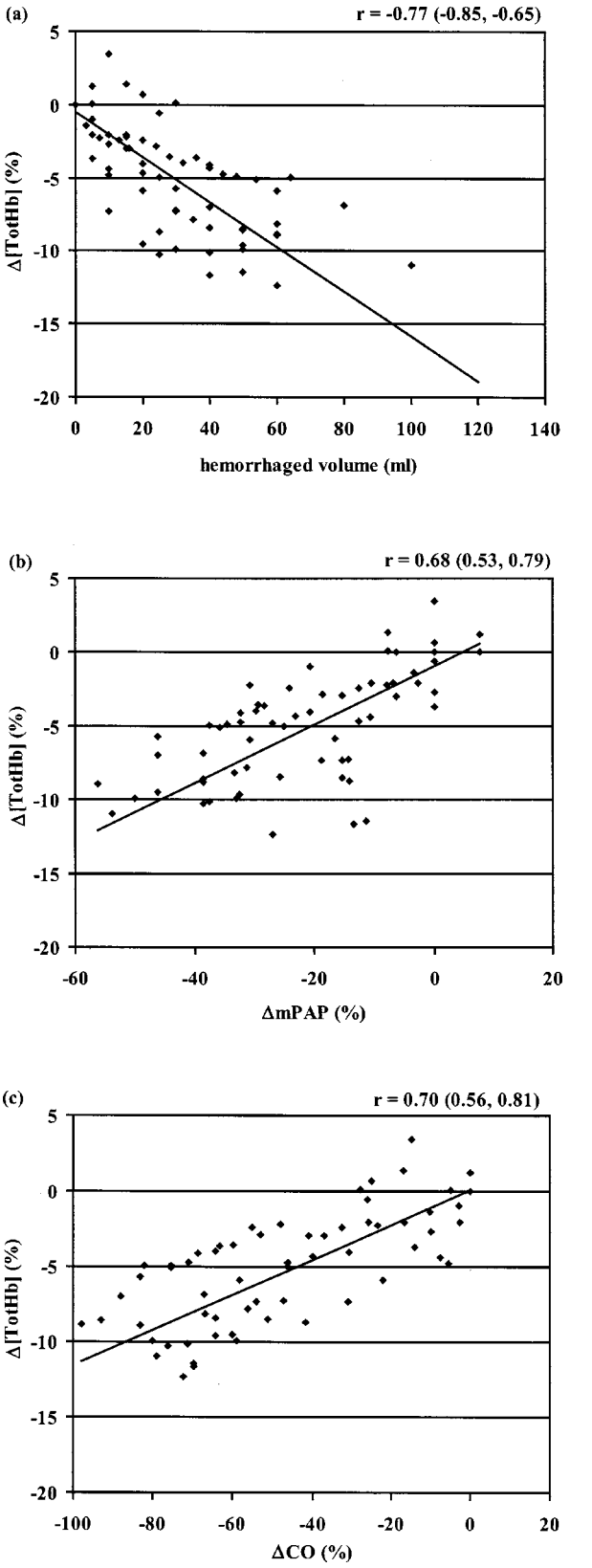

Fig. 5 FDPM-derived Δ[TotHb] vs (a) HV, (b) ΔmPAP, and (c) ΔCO. Correlation coefficient (*r*) and 95% confidence intervals for the data are shown in (a)–(c). All data from animals in the hypovolemic group are combined.

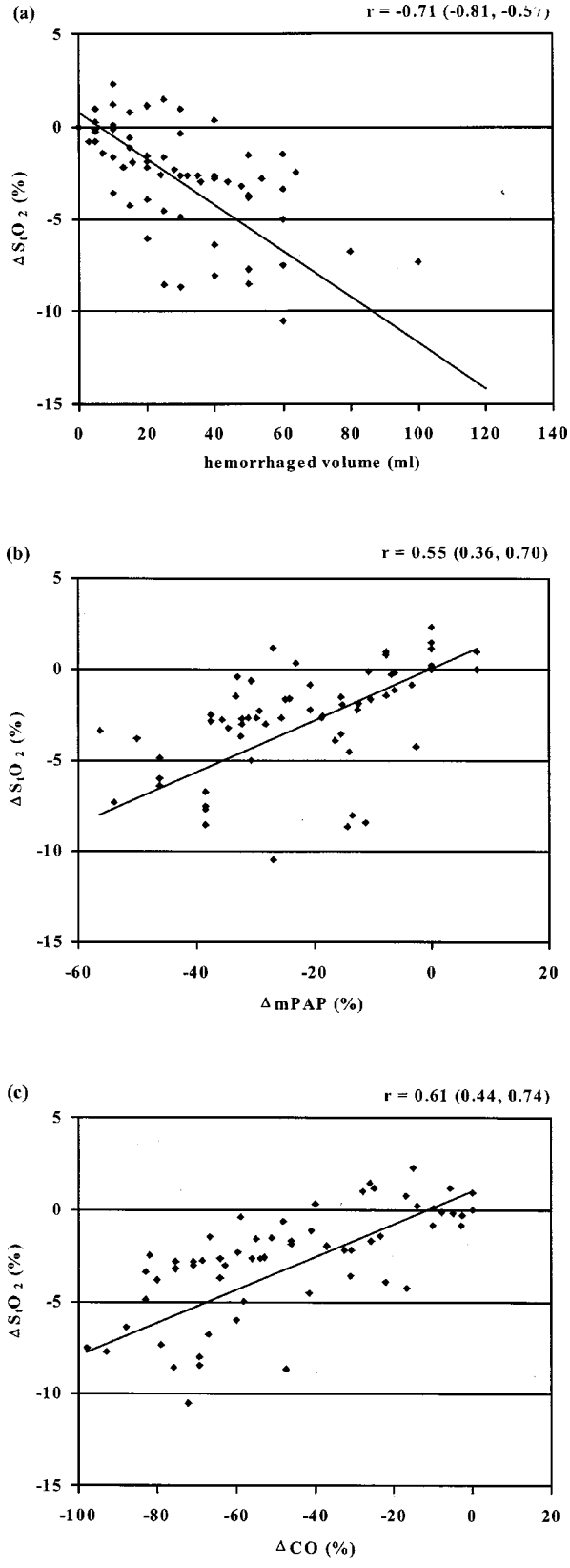

Fig. 6 FDPM-derived ΔS_tO_2 vs (a) HV, (b) ΔmPAP, and (c) ΔCO. Correlation coefficient (*r*) and 95% confidence intervals for the data are shown in (a)–(c). All data from animals in the hypovolemic group are combined.

correlation coefficients and 95% confidence interval for the associations of Δ[TotHb] and ΔS_tO_2 vs HV, ΔmPAP, and ΔCO.

3.4 Dobutamine

Dobutamine increased the CO and mPAP in a dose dependent manner as shown in Figure 7(a). Cardiac output increased by ~16% and ~32% in response to dobutamine doses of 30 and 40–50 μg/kg, respectively. Likewise, dobutamine doses of 30 and 40–50 μg/kg increased mPAP ~25% and ~35%, respectively. Figure 7(b) shows the mean changes in [TotHb] and S_tO_2 in response to administration of dobutamine. The [TotHb] measured increased ~2% and ~2.5% in response to dobutamine doses of 30 and 40–50 μg/kg, respectively, while S_tO_2 increased ~0.5% for doses between 30 and 50 μg/kg. The percentages of change in [TotHb] and S_tO_2 were compared to the dobutamine-mediated increase in CO and mPAP. Figures 8(a) and 8(b) show Δ[TotHb] vs ΔCO and ΔS_tO_2 vs ΔCO, respectively. A correlation coefficient of 0.70 was observed for Δ[TotHb] vs ΔCO. As shown in Figure 8 [TotHb] increased approximately 4% in response to a 50% increase in CO. This rate is slightly less than but comparable to the percentages of change in [TotHb] in response to a hypovolemia-mediated decrease in CO, where [TotHb] decreased ~6% in response to a decrease of 50% in CO. The correlation between ΔS_tO_2 vs ΔCO yielded a considerably smaller value of 0.42. Mixed S_tO_2 increased by less than 1% in response to a dobutamine-mediated increase of 50% in CO. This is considerably less than the changes in S_tO_2 due to the hypovolemia-mediated decrease in CO, where S_tO_2 decreased ~4% in response to a 50% decrease in CO. The correlation coefficients for Δ[TotHb] vs ΔmPAP or for ΔS_tO_2 vs ΔmPAP were 0.30 and 0.17, respectively. Table 5 summarizes the correlation coefficients and 95% confidence intervals for statistically significant associations in the dobutamine study.

4 Discussion and Conclusion

Acute hypovolemia is the leading cause of shock.[6,28] Early identification of impending tissue hypoxia accompanied by rapid intervention constitutes the most effective way in which to prevent organ failure.[29,30] Presently, the recommended strategy for identifying hypovolemic shock is to assess the clinical signs and symptoms, central blood volume, cardiac output, arterial blood chemistry, and systemic blood pressure.[3,31] Pulmonary wedge pressure (PWP) has been shown to be a sensitive and accurate indicator of central blood volume;[32] low PWP means that the preload volume is insufficient to maintain adequate cardiac output. However, measurements of PWP necessitate invasive monitoring devices that include placing a balloon catheter through the right ventricle into the pulmonary artery. Some of the potential complications of PWP measurements include infection, the rupture of veins, embolisms, and pneumothorax.[33,34] Pulmonary artery thermodilution catheterization is the most commonly accepted method for measuring CO in a clinical setting.[35–37] Like PWP measurements, the procedure is invasive. Doppler ultrasound is a noninvasive alternative for measuring cardiac output.[38] However, Doppler ultrasound is less accurate than invasive procedures, it cannot be accurately obtained in many cases, it requires a highly experienced operator, and it cannot

Table 4 Summary of the statistically significant correlations between ΔmPAP and ΔCO versus HV as well as correlation among Δ[TotHb] and ΔS_tO_2 vs HV, ΔmPAP, and ΔCO during hypovolemia.

Parameters to be correlated	Correlation coefficient r [a]	95% confidence interval (lower limit, upper limit)[a]
ΔmPAP (%) vs HV (mL)	–0.76	(–0.84, –0.63)
ΔCO (%) vs HV (mL)	–0.82	(–0.88, –0.72)
ΔTotHb (%) vs. HV (mL)	–0.77	(–0.85, –0.65)
ΔTotHb (%) vs ΔmPAP (%)	0.68	(0.53, 0.79)
ΔTotHb (%) vs ΔCO (%)	0.70	(0.56, 0.81)
ΔS_tO_2 (%) vs HV (mL)	–0.71	(–0.81, –0.57)
ΔS_tO_2 (%) vs ΔmPAP (%)	0.55	(0.36, 0.70)
ΔS_tO_2 (%) vs ΔCO (%)	0.61	(0.44, 0.74)

[a] All data from the hypovolemic group were combined, $n = 68$ data points.

be used for continuous monitoring.[39] Near real-time magnetic resonance imaging is potentially an ideal modality by which to quantify cardiac output as well as to assess anatomical features of the heart. Presently, the use of magnetic resonance imaging for cardiac output measurements is expensive, and is not practical for unstable patients or for frequent serial assessments.

Systemic blood pressure and arterial hemoglobin oxygen saturation (S_aO_2) are noninvasive measurements, but are not sensitive indicators of tissue perfusion and oxygenation. Reflex mechanisms, such as systemic vasoconstriction and increased cardiac output can maintain nearly constant blood pressure when faced with severe hypovolemia. Thus, blood pressure decompensation often indicates that shock has progressed or advanced to irreversible stages of organ damage.[3] Because S_aO_2 represents the oxygenation state of arterial blood, it is an indicator of the oxygen exchange processes of the lung, not of the oxygenation status of local tissues nor a measure of the delivery of oxygen to tissues. Although the product of S_aO_2 and CO is a good indicator of the delivery of whole body oxygen, it is only an indirect measure of local tissue oxygenation because regional levels depend on the O_2 distribution as well as utilization. In fact, many of the current physiologic measures (CO, PWP, S_aO_2, etc.) primarily indicate the perfusion and oxygenation status of the whole body. These whole body hemodynamic parameters may poorly represent delivery of oxygen and utilization of certain organs.[40,41] Percutaneous oxygen electrodes measure tissue oxygenation in the local milieu of the sensor.[42] However, electrode-based measurements often reflect the oxygenation status of superficial tissues, they are locally invasive, and they are unreliable *in vivo* for a variety of reasons. Consequently, a noninvasive method that assesses the local tissue oxygen status and, at the same time, correlates to standard hemodynamic parameters is of great clinical interest.[4,29,43]

FDPM-derived physiologic properties [TotHb] and S_tO_2 are direct indicators of the status of local tissue oxygenation. [TotHb] represents hemoglobin in the arteries, capillaries, and veins of tissues at the measurement site. Likewise, S_tO_2 quan-

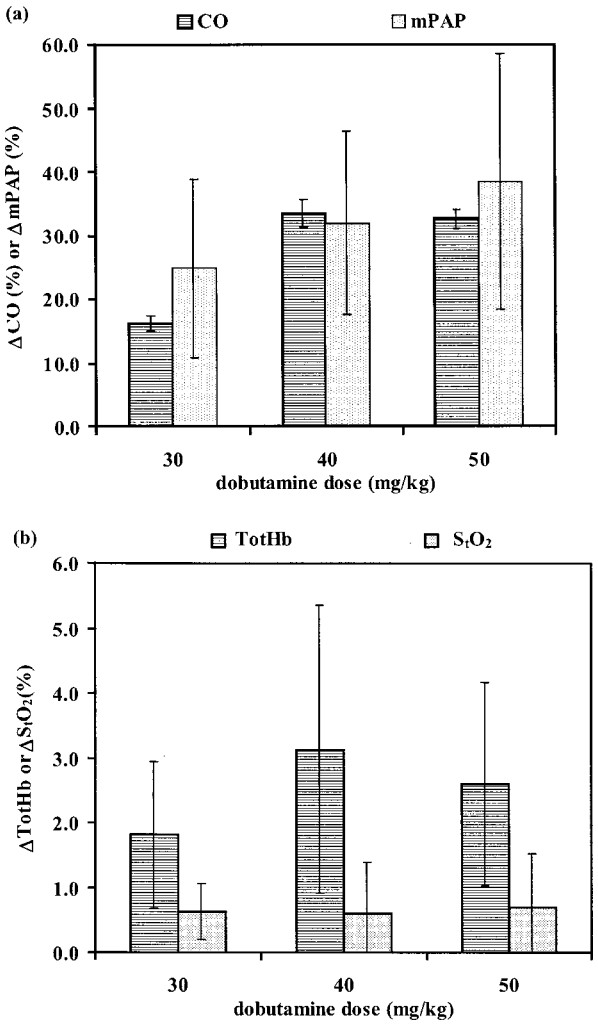

Fig. 7 Changes in hemodynamic- and FDPM-derived physiologic parameters in response to dobutamine: (a) ΔCO and ΔmPAP vs the dobutamine dose. (b) Δ[TotHb] and ΔS_tO_2 vs the dobutamine dose. All parameters, except for ΔS_tO_2, show dose-dependent responses. All data from animals in the dobutamine-treated group are combined.

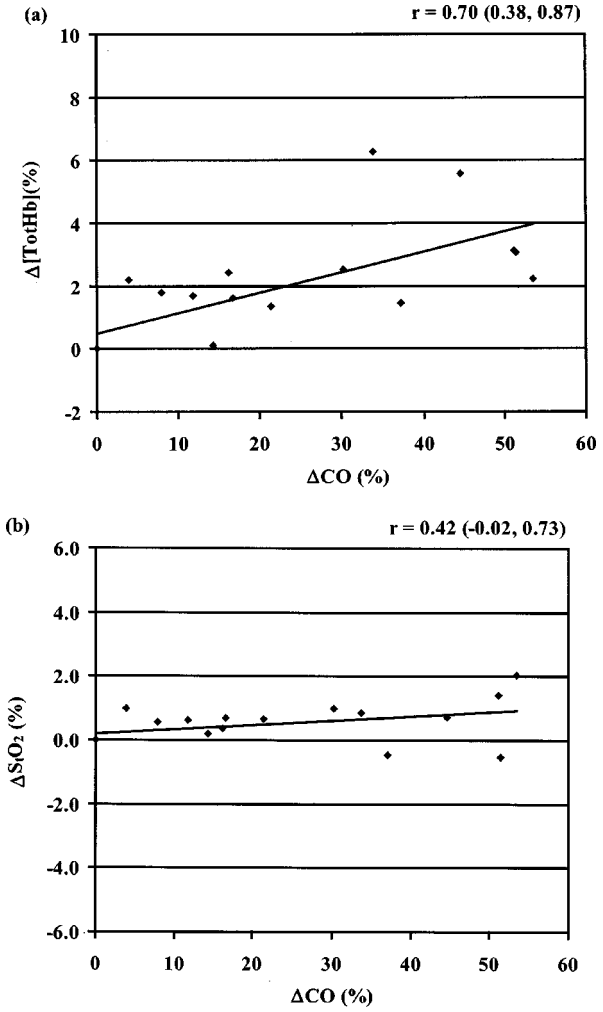

Fig. 8 FDPM-derived Δ[TotHb] and ΔS_tO_2 vs the dobutamine-mediated increase in CO: (a) Δ[TotHb] vs ΔCO and (b) ΔS_tO_2 vs ΔCO. Correlation coefficient (*r*) and 95% confidence intervals for the data are shown in (a) and (b). All data from animals in the dobutamine-treated group are combined.

tifies the mixed arterial-venous oxygen saturation of local tissues. [TotHb] and S_tO_2 values depend not only on the delivery of oxygen but also on utilization of local tissue oxygen. [TotHb] decreases in proportion to a reduction in delivery (DO_2) of regional oxygen. Vasoconstriction and decreased hematocrit are likely to accompany the lowering of [TotHb]. Mixed tissue saturation, i.e., S_tO_2, decreases when the utilization of oxygen exceeds delivery. In fact, FDPM-derived [TotHb] and S_tO_2 have experimentally been shown to be sensitive to changes in tissue perfusion and oxygenation.[17,25,44] Moreover, [TotHb] and S_tO_2 may also be sensitive to perturbations in CO, PWP, and S_aO_2, since these parameters clearly affect local tissue oxygenation.

The measurements of CO and mPAP during administration of dobutamine were consistent with the known pharmacological effects of dobutamine on the circulatory system. Dobutamine increases cardiac output and elevates pulmonary artery pressure.[45,46] Our results show that dobutamine increased CO and mPAP in a dose-dependent manner (Figure 7). Analysis of the dobutamine data indicates that FDPM-derived [TotHb] and S_tO_2 are statistically correlated with dobutamine-mediated changes in CO. The dobutamine-mediated changes in CO are comparable to the sensitivity of [TotHb] to hypovolemia-mediated changes in CO. Interestingly, the sensitivity of ΔS_tO_2 to dobutamine-mediated ΔCO was considerably lower than its sensitivity to hypovolemia-induced ΔCO. Specifically, S_tO_2 increased 1% per 50% increase in dobutamine-mediated ΔCO, while S_tO_2 decreased 4% in response to a 50% decrease in hypovolemia-mediated ΔCO. A plausible explanation may be that hypovolemia causes intense stress not found in the administration of dobutamine. First, hypovolemia caused systemic vasoconstriction and cardiac output may be preferentially shunted away from the region of the skin to the vital organs, thereby exaggerating the decrease of S_tO_2 in the periphery. Second, tissues may enter hypercatabolic states in response to ischemia, leading to maximal extraction of oxygen from arterial and venous blood as well as causing acidosis. Both factors contribute to the heightened S_tO_2 sensitivity to CO perturbation observed during hypovolemic shock. In the case of the administration of dobutamine the delivery of oxygen exceeds the demand. The excess oxygen contributes to an increase in S_tO_2, but the tissues' oxygen saturation clearly does not change to the degree observed in hypovolemia.

FDPM technology is capable of separately measuring μ_a and μ_s'. So far, little is known about the effect(s) of perfusion changes on tissue μ_s'. In this study, tissue μ_s' did not show statistically significant changes in response to hemodynamic

Table 5 Summary of the statistically significant correlations among dose, Δ[TotHb], and ΔS_tO_2 vs ΔCO and ΔmPAP during administration of dobutamine.

Parameters to be correlated	Correlation coefficient *r*[a]	95% confidence interval (lower limit, upper limit)[a]
ΔCO (%) vs dose (mg/kg)	0.74	(0.44, 0.89)
ΔmPAP (%) vs dose (mg/kg)	0.56	(0.16, 0.80)
ΔTotHb (%) vs ΔCO (%)	0.70	(0.38, 0.87)
ΔS_tO_2 (%) vs ΔCO (%)	0.42	(–0.02, 0.73)

[a] All data from the dobutamine-treated group were combined, $n = 20$ data points.

manipulations. This observation is consistent with the fact that FDPM measurements were performed during the acute phase of tissue ischemia. Because μ_s' depends mainly on the tissues' structural milieu,[20,21] it may be sensitive to long-term pathophysiologic processes that alter tissue architecture, including cellular swelling, reperfusion injury, tissue necrosis, and wound healing. These processes do not occur during acute hypovolemia, which may explain why μ_s' was unperturbed following acute hemorrhaging or administration of dobutamine.

In summary, the results from this pilot study using a rabbit model indicate that the quantitative, FDPM-derived [TotHb] and S_tO_2 values statistically correlate with blood loss as well as to hypovolemia- and dobutamine-mediated perturbations in CO and mPAP. Significant is the fact that [TotHb] and S_tO_2 are responsive to (1) blood loss of as little as ~7% and (2) changes in mPAP and CO of as little as 15%. These results suggest that [TotHb] and S_tO_2 may be used to noninvasively identify impending hypovolemic shock and to monitor the efficacy of therapeutic interventions, such as restoration of the blood volume and administration of dobutamine. Although we have specifically addressed hypovolemic shock in this study, noninvasive FDPM spectroscopy may also be useful for other clinical manifestations associated with tissue hypoxia, such as peripheral vascular disease[47] and septic or cardiogenic shock. FDPM technology warrants further investigation in surgical and critical care settings where quantitative, dynamic monitoring of local tissue oxygenation would be of vital clinical importance.

Acknowledgments

The authors would like to thank Terry Waite-Kennedy and Laurie Newman for their assistance with animal care. This work was supported by the National Institutes of Health (NIH), National Center for Research Resources (NCRR), Laser Microbeam and Medical Program (Grant No. RR-01192), NIH Grant No. R29-GM50958, Department of Energy (DOE Grant No. DE-FG03-91ER61227), Office of Naval Research (ONR Grant No. N00014-91-C-0134), California Tobacco Related Disease Research Program (CTRDRP Grant No. 6RT-0158), and American Lung Association (ALA Grant No. CI-0303-N). One of the authors (T.H.P.) is grateful for support by a Whitaker Foundation Biomedical Engineering graduate fellowship. A second author (R.H.) wishes to acknowledge the Swiss National Research Foundation, the Huggenberger-Bischoff Stiftung, and the Theodor und Ida Herzog-Egli Stiftung.

References

1. A. C. Guyton and J. E. Hall, *Cardiovascular Physiology IV*, University Park Press, Baltimore, Maryland (1982).
2. E. Schlichting and T. Lyberg, ''Monitoring of tissue oxygenation in shock: An experimental study in pigs,'' *Crit. Care Med.* **23**, 1703–1710 (1995).
3. R. S. Irwin, F. B. Cerra, and J. M. Rippe, *Irwin and Rippe's Intensive Care Medicine*, Lippincott–Raven, Philadelphia (1999).
4. W. C. Shoemaker, H. B. Kram, and P. L. Appel, ''Therapy of shock based on pathophysiology, monitoring, and outcome prediction,'' *Crit. Care Med.* **18**, S19–S25 (1990).
5. M. E. Astiz and E. C. Rackow, ''Assessing perfusion failure during circulatory shock,'' *Crit. Care Clin.* **9**, 299–312 (1993).
6. W. C. Shoemaker, C. C. Wo, D. Demetriades, H. Belzberg, J. A. Asensio, E. E. Cornwell, J. A. Murray, T. V. Berne, J. Adibi, and R. S. Patil, ''Early physiologic patterns in acute illness and accidents: Toward a concept of circulatory dysfunction and shock based on invasive and noninvasive hemodynamic monitoring,'' *New Horiz.* **4**, 395–412 (1996).
7. D. L. Liu, K. Svanberg, I. Wang, S. Andersson-Engels, and S. Svanberg, ''Laser Doppler perfusion imaging: New technique for determination of perfusion and reperfusion of splanchnic organs and tumor tissue,'' *Lasers Surg. Med.* **20**, 473–479 (1997).
8. J. A. Wahr, K. K. Tremper, S. Samra, and D. T. Delpy, ''Near-infrared spectroscopy: Theory and applications,'' *J. Cardiothorac Vasc. Anesth.* **10**, 406–418 (1996).
9. R. A. De Blasi, M. Ferrari, M. Antonelli, G. Conti, N. Almenreader, and A. Gasparetto, ''O_2 consumption-O_2 delivery relationship and arteriolar resistance in the forearm of critically ill patients measured by near infrared spectroscopy,'' *Shock* **6**, 319–325 (1996).
10. C. J. Aldrich, D. D'Antona, J. A. Spencer, J. S. Wyatt, D. M. Peebles, and D. T. Delpy, ''The effect of maternal pushing on fetal cerebral oxygenation and blood volume during the second stage of labour,'' *Br. J. Obstet. Gynaecol.* **102**, 448–453 (1995).
11. T. Hamaoka, H. Iwane, T. Shimomitsu, T. Katsumura, N. Murase, S. Nishio, T. Osada, Y. Kurosawa, and B. Chance, ''Noninvasive measures of oxidative metabolism on working human muscles by near-infrared spectroscopy,'' *J. Appl. Physiol.* **81**, 1410–1417 (1996).
12. B. Chance, ''Near-infrared images using continuous, phase-modulated, and pulsed light with quantitation of blood and blood oxygenation,'' *Ann. N.Y. Acad. Sci.* **838**, 29–45 (1998).
13. D. M. Mancini, L. Bolinger, H. Li, K. Kendrick, B. Chance, and T. Wilson, ''Validation of near-infrared spectroscopy in humans,'' *J. Appl. Physiol.* **77**, 2740–2747 (1994).
14. R. Wariar, J. N. Gaffke, R. G. Haller, and L. A. Bertocci, ''A modular NIRS system for clinical measurement of impaired skeletal muscle oxygenation,'' *J. Appl. Physiol.* **88**, 315–325 (2000).
15. M. S. Patterson, B. Chance, and B. C. Wilson, ''Time resolved reflectance and transmittance for the non-invasive measurement of optical properties,'' *Appl. Opt.* **28**, 2331–2336 (1989).
16. B. J. Tromberg, R. C. Haskell, S. J. Madsen, and L-O. Svaasand, ''Characterization of tissue optical properties using photon density waves,'' *Comments Mol. Cell. Biophys.* **8**, 359–386 (1995).
17. R. Hornung, T. H. Pham, K. A. Keefe, M. W. Berns, Y. Tadir, and B. J. Tromberg, ''Quantitative near-infrared spectroscopy of cervical dysplasia *in vivo*,'' *Hum. Reprod.* **14**, 2908–2916 (1999).
18. M. Cope, Ph.D. thesis, University College, London (1991).
19. F. A. Duck, *Physical Properties of Tissue*, Academic, London (1990).
20. I. S. Saidi, S. L. Jacques, and F. K. Tittel, ''Mie and Rayleigh modeling of visible-light scattering in neonatal skin,'' *Appl. Opt.* **34**, 7410–7418 (1995).
21. J. R. Mourant, J. P. Freyer, A. H. Hielscher, A. A. Eick, D. Shen, and T. M. Johnson, ''Mechanisms of light scattering from biological cells relevant to noninvasive optical-tissue diagnostics,'' *Appl. Opt.* **37**, 3586–3593 (1998).
22. D. L. Liu, S. Andersson-Engels, C. Sturesson, K. Svanberg, C. H. Håkansson, and S. Svanberg, ''Tumour vessel damage resulting from laser-induced hyperthermia alone and in combination with photodynamic therapy,'' *Cancer Lett.* **111**, 157–165 (1996).
23. M. K. Fehr, B. J. Tromberg, L. O. Svaasand, P. Ngo, M. W. Berns, and Y. Tadir, ''Structural and functional effects of endometrial photodynamic therapy in a rat model,'' *Am. J. Obstet. Gynecol.* **175**, 115–121 (1996).
24. T. H. Pham, O. Coquoz, J. B. Fishkin, E. Anderson, and B. J. Tromberg, ''A broad bandwidth frequency domain instrument for quantitative tissue optical spectroscopy,'' *Rev. Sci. Instrum.* **71**, 2500–2513 (2000).
25. J. B. Fishkin, O. Coquoz, E. R. Anderson, M. Brenner, and B. J. Tromberg, ''Frequency-domain photon migration measurements of normal and malignant tissue optical properties in a human subject,'' *Appl. Opt.* **36**, 10–20 (1997).
26. B. J. Tromberg, L. O. Svaasand, T.-T. Tsay, and R. C. Haskell, ''Properties of photon density waves in multiple-scattering media,'' *Appl. Opt.* **32**, 607–616 (1993).
27. C. L. Lawson and R. J. Hanson, *Solving Least Squares Problems*, Prentice–Hall, New York (1974).
28. N. J. Thomas and J. A. Carcillo, ''Hypovolemic shock in pediatric patients,'' *New Horiz* **6**, 120–129 (1998).
29. W. C. Shoemaker, ''Oxygen transport and oxygen metabolism in shock and critical illness. Invasive and noninvasive monitoring of

circulatory dysfunction and shock,'' *Crit. Care Clin.* **12**, 939–969 (1996).
30. W. C. Shoemaker, A. B. Peitzman, R. Bellamy, R. Bellomo, S. P. Bruttig, A. Capone, M. Dubick, G. C. Kramer, J. E. McKenzie, P. E. Pepe, P. Safar, R. Schlichtig, J. W. Severinghaus, S. A. Tisherman, and L. Wiklund, ''Resuscitation from severe hemorrhage,'' *Crit. Care Med.* **24** S12–S23 (1996).
31. L. D. Britt, L. J. Weireter, J. L. Riblet, J. A. Asensio, and K. Maull, ''Priorities in the management of profound shock,'' *Surg. Clin. North Am.* **76**, 645–660 (1996).
32. M. Lichtwarck-Aschoff, R. Beale, and U. J. Pfeiffer, ''Central venous pressure, pulmonary artery occlusion pressure, intrathoracic blood volume, and right ventricular end-diastolic volume as indicators of cardiac preload,'' *J. Crit. Care* **11**, 180–188 (1996).
33. C. G. Elliott, G. A. Zimmerman, and T. P. Clemmer, ''Complications of pulmonary artery catheterization in the care of critically ill patients. A prospective study,'' *Chest* **76**, 647–658 (1979).
34. T. Coulter and H. Wiedemann, ''Complications of hemodynamic monitoring,'' *Clin. Chest Med.* **20**, 249–267 (1999).
35. R. M. Sade, A. A. Richi, and J. P. Dearing, ''Calculation of systemic blood flow with pulmonary artery thermistor probe,'' *J. Thorac. Cardiovasc. Surg.* **78**, 576–578 (1979).
36. K. G. Lehman and M. S. Platt, ''Improved accuracy and precision of thermodilution cardiac output measurement using a dual thermistor catheter system,'' *J. Am. Coll. Cardiol.* **33**, 883–891 (1999).
37. C. Zöllner, J. Polasek, E. Kilger, B. Pichler, U. Jaenicke, J. Briegel, H. O. Vetter, and M. Haller, ''Evaluation of a new continuous thermodilution cardiac output monitor in cardiac surgical patients: A prospective criterion standard study,'' *Crit. Care Med.* **27**, 293–298 (1999).
38. C. M. Moran, W. N. McDicken, P. R. Hoskins, and P. J. Fish, ''Developments in cardiovascular ultrasound. Part 3. Cardiac applications,'' *Med. Biol. Eng. Comput.* **36**, 529–543 (1998).
39. P. S. Douglas and M. J. Frey, ''Assessment of anatomy and cardiac function by Doppler echocardiography,'' *Cardiol. Clin.* **7**, 483–491 (1989).
40. D. R. Chittock and J. Russell, ''Oxygen delivery and consumption during sepsis,'' *Clin. Chest Med.* **17**, 263–278 (1996).
41. A. C. Guyton and J. E. Hall, *Human Physiology and Mechanisms of Disease*, Saunders, London (1997).
42. F. Moore and J. Haenel, ''Advances in oxygen monitoring of trauma patients,'' *Med. Instrum.* **22**, 135–142 (1988).
43. J. A. Asensio, D. Demetriades, T. V. Berne, and W. C. Shoemaker, ''Invasive and noninvasive monitoring for early recognition and treatment of shock in high-risk trauma and surgical patients,'' *Surg. Clin. North Am.* **76**, 986–997 (1996).
44. B. J. Tromberg, O. Coquoz, J. B. Fishkin, T. Pham, E. R. Anderson, J. Butler, M. Cahn, J. D. Gross, V. Venugopalan, and D. Pham, ''Noninvasive measurements of breast tissue optical properties using frequency-domain photon migration,'' *Philos. Trans. R. Soc. London, Ser. B* **352**, 661–668 (1997).
45. E. H. Sonnenblick, W. H. Frishman, and T. H. LeJemtel, ''Dobutamine: A new synthetic cardioactive sympathetic amine,'' *N. Engl. J. Med.* **300**, 17–22 (1979).
46. D. McCaig and J. R. Parratt, ''The cardiovascular pharmacology of 7-propyl-theo-phylline-dopamine (D4975): Comparison with dopamine and dobutamine,'' *Br. J. Pharmacol.* **67**, 239–245 (1979).
47. E. Gratton, S. Fantini, M. A. Franceschini-Fantini, G. Gratton, and M. Fabiani, ''Measurements of scattering and absorption changes in muscle and brain,'' *Philos. Trans. R. Soc. London, Ser. B* **352**, 727–735 (1997).